Refinement of Repeated β-turn Structure for Silk I Conformation of *Bombyx mori* Silk Fibroin Using ^{13}C Solid-State NMR and X-ray Diffraction Methods

Tetsuo Asakura,* Kosuke Ohgo, Kohei Komatsu, Masakazu Kanenari, and Kenji Okuyama

Department of Biotechnology, Tokyo University of Agriculture and Technology, Koganei, Tokyo 184-8588, Japan

Received May 4, 2005; Revised Manuscript Received June 18, 2005

ABSTRACT: Refinement of the structural model of silk I (the structure of *Bombyx mori* silk fibroin before spinning in the solid state) proposed previously was performed on the basis of a detailed analysis of the ^{13}C solid-state NMR data using two-dimensional (2D) spin-diffusion NMR and REDOR of stable isotope-labeled $(AG)_{15}$, coupled with the X-ray diffraction analysis of the crystalline fraction of *B. mori* silk fibroin. The repeated β-turn type II structure was proposed, with the torsion angles $(\phi, \psi) = (-62°, 125°)$ for Ala residue and $(\phi, \psi) = (77°, 10°)$ for Gly residue of poly(Ala-Gly) chain, which satisfies both solid-state NMR and X-ray diffraction data quantitatively. The torsion angles determined in this work were slightly different from the previous angles, $(\phi, \psi) = (-60°, 130°)$ for Ala residue and $(\phi, \psi) = (70°, 30°)$ for Gly residue. The intra- and intermolecular hydrogen bonding was formed alternatively along the chain. The solid-state NMR is sensitive to the local conformation of a chain, but X-ray diffraction is rather sensitive to intermolecular arrangement as well as the conformation. Thus, the detailed silk I structure with intermolecular arrangement was determined by the use of several solid-state NMR and X-ray diffraction methods complementarily.

Introduction

It is remarkable that silk fibroin from *Bombyx mori* silkworms can produce strong, tough fibers at room temperature and from an aqueous solution.[1] Thus, it is important to know the structure of the silk fibroin before spinning, to elucidate the mechanism of fiber formation and design new silk-like materials that can be produced under similar mild conditions.

The amino acid composition (in mol %) of *B. mori* silk fibroin showed the predominance of five amino acids: Gly (42.9%), Ala (30.0%), Ser (12.2%), Tyr (4.8%) and Val (2.5%).[2] By using the cDNA sequencing method, Mita *et al.*[3] and later Zhou et al.,[4] employing shotgun sequencing strategy combined with traditional physical map directed sequencing of the fibroin gene of the heavy chain, predicted the presence of unusual repeat sequences in the silk fibroin. The two crystalline forms, silk I and silk II, have been reported as the dimorphs of *B. mori* silk fibroin, on the basis of extensive investigations from X-ray diffraction,[5−10] electron diffraction,[7,8,10] conformational energy calculation,[11] infrared,[12] and ^{13}C and ^{15}N solid-state NMR spectroscopy.[12−20] In the structural analysis of *B. mori* silk fibroin, poly(alanyl-glycine) (poly(AG)) or alanyl-glycine copolypeptide $(AG)_n$ has been used for spectroscopic studies as the model system. In our previous papers,[21,22] we found that the ^{13}C peaks of the Ala Cβ positions in the CP/MAS NMR spectra of both *B. mori* silk fibroin fiber and $(AG)_{15}$ in the silk II form are broad and asymmetric, which reflects a heterogeneous structure. The relative proportions of the various heterogeneous components were determined from their relative peak intensities after line-shape deconvolution.

* Author to whom correspondence should be addressed. E-mail: asakura@cc.tuat.ac.jp. Telephone and Fax: (+81)-423-83-7733.

On the other hand, silk I structure appears when *B. mori* silk fibroin stored in the silk gland is dried gently.[1] Namely, the CD pattern of silk fibroin at low concentration, ~0.1%, may indicate that the predominant structure is random coil/unordered. At a significantly higher concentration, ~8.6%, a distinct CD pattern with poorly defined troughs, at ~218 and ~206 nm, was observed, indicating that the appearance of some ordered structure, that is, silk I.[23−25] This is also supported from the ORD measurements by changing the concentration of liquid silk from the silkworm; the observation of the b_0 value, which reflects the fraction of helical structure, indicates that the helical contents start increasing from 5% of silk concentration and reaches 40% helical contents in the liquid silk obtained from the middle silk gland (silk fibroin concentration ~30%).[24] It is noted that the ^{13}C CP/MAS NMR chemical shifts of Ala Cα, Cβ, and C=O carbons of *B. mori* silk fibroin with silk I formed in the solid state are almost similar to the ^{13}C chemical shifts of these Ala carbons of the silk fibroin in solution state (liquid silk obtained from the middle silk gland).[23−25] This means that the structure is basically the same between these silk fibroin samples because ^{13}C chemical shifts of the Ala carbons show strong conformation dependence.[12−16]

Despite a long history of interest in the silk I structure in the solid state, it largely remained poorly understood.[7,9] We recently attempted the characterization of the molecular structure of the silk I form using the synthetic peptide $(AG)_{15}$ sequence as a model for the highly repetitive crystalline domain of the fibroin.[26−28] The proposed model incorporated repeated type II β-turn structure, stabilized by a typical 4→1 intramolecular hydrogen bond.

In this paper, refinement of repeated β-turn structure for silk I conformation proposed previously[26] was performed on the basis of a more detailed analysis of the

10.1021/ma050936y CCC: $30.25
Published on Web 07/19/2005

Table 1. ^{13}C, ^{15}N Double-Labeled Peptides for REDOR Experiment[a]

peptide	observed, (Å)[b]	calculated, (Å)[c]
R1: AGAGAGAGAGAGAG[^{15}N]A^{15}[2-^{13}C]G^{16}AGAGAGAGAGAGAG	4.7 ± 0.1	4.7
R2: AGAGAGAGAGAGAGA[^{15}N]G^{15}[2-^{13}C]A^{17}GAGAGAGAGAGAG	4.3 ± 0.1	4.2
R3: AGAGAGAGAGAGA[1-^{13}C]G^{14}A[^{15}N]G^{16}AGAGAGAGAGAGAG	3.8 ± 0.1	3.7
R4: AGAGAGAGAGAGAGAG[1-^{13}C]A^{15}G[^{15}N]A^{17}GAGAGAGAGAGAG	3.2 ± 0.1	3.2
R5: AGAGAGAGAGAGA[1-^{13}C]G^{14}AG[^{15}N]A^{17}GAGAGAGAGAGAG	4.0 ± 0.1	3.9
R6: AGAGAGAGAGAGAG[^{15}N]A^{15}[1-^{13}C]G^{16}AGAGAGAGAGAGAG	5.0 ± 0.1	5.1
R7: AGAGAGAGAGAGA[^{15}N]G^{14}AG[3-^{13}C]A^{17}GAGAGAGAGAGAG	5.8 ± 0.3	5.7

[a] The observed and calculated atomic distances between ^{13}C and ^{15}N labeled sites were also listed. [b] The ^{13}C-^{15}N distances for R3, R4, and R5 were reported previously.[26] [c] The ^{13}C-^{15}N distances were calculated according to the β-turn type II structure as the model for silk I obtained here.

^{13}C solid-state NMR data, that is, two-dimensional (2D) spin-diffusion NMR and REDOR results of stable, isotope-labeled $(AG)_{15}$, coupled with the X-ray diffraction analysis of the crystalline fraction of *B. mori* silk fibroin.

Materials and Methods

1. REDOR Experiment. As summarized in Table 1, seven ^{13}C, ^{15}N double-labeled $(AG)_{15}$ peptides with different labeling positions were synthesized with solid-phase methods for REDOR experiments.[29] The three REDOR data, R3, R4, and R5, were already published.[26] The peptides $(AG)_{15}$ were dissolved in 9 M LiBr and then dialyzed against water for 4 days. The precipitated samples were collected and dried. The structures of all peptides were silk I, which was confirmed from the IR and ^{13}C CP/MAS NMR spectra. The REDOR experiments were performed on a Chemagnetics Infinity 400 MHz spectrometer at 9.4 T (100.0 MHz for ^{13}C and 40.3 MHz for ^{15}N) using the following conditions: a 4-mm triple-channel magic-angle probe; spinning rate 6.666 kHz; π pulses for ^{13}C and ^{15}N channels, respectively, 6.5 and 8.2 μs; recycle delay 3.0 s. Phases of ^{15}N π pulses were cycled according to the XY-8 scheme[29] to minimize off-resonance and pulse-error effects. REDOR evolution times ranged up to 18 ms. Values of $\Delta S/S_0 = 1 - S/S_0$ were computed as the ratios of peak intensities in the REDOR spectra.

2. Analysis of 2D Spin-Diffusion NMR Spectrum. The 2D spin-diffusion NMR spectra of $(AG)_6A[1\text{-}^{13}C]G^{14}[1\text{-}^{13}C]A^{15}G(AG)_7$, $(AG)_7[1\text{-}^{13}C]A^{15}[1\text{-}^{13}C]G^{16}(AG)_7$, and $(AG)_6A[1\text{-}^{13}C]G^{14}A[1\text{-}^{13}C]G^{16}(AG)_7$ observed for determination of the torsion angles of Ala (ϕ, ψ) and Gly (ϕ, ψ) residues published previously[26] are used for the refinement of the torsion angles of these residues. The RMSD value as functions of ϕ and ψ values was newly introduced to quantify the difference between the observed and calculated spectra. The definition of the RMSD was

$$\mathrm{RMSD}(\phi,\psi) = \sqrt{\frac{\sum_{i=1}^{N}[E_i - \lambda(\phi,\psi)\,S_i(\phi,\psi)]^2}{N}}$$

where N is the number of intensities analyzed, E_i are the experimental intensities, $S_i(\phi,\psi)$ are the calculated intensities, and $\lambda(\phi,\psi)$ is a scaling factor calculated to minimize RMSD at each (ϕ,ψ) pair.[30] For simulation of 2D spin-diffusion NMR spectra, the calculations were performed using a grid of 15° for ϕ and ψ values. Visualization of spectra and RMSD calculation were performed using MATLAB (The MathWorks, Inc.).

3. Packing Models and Their Refinement. The most plausible space group and the number of a chemical repeating unit of Ala-Gly in a unit cell were reported to be $P2_12_12_1$ and four ($Z = 4$), respectively.[9] For packing four chemical repeating units in a unit cell, the 2_1-helical axis of the molecule should coincide with the crystallographic 2_1-axis parallel to the c direction. For positioning the molecular model in the unit cell, two additional parameters were used to define the relative axial rotation and translation along the c axis. For refinement of the structure, we sought to minimize the quantity Ω in the following least-squares fashion:[31]

$$\Omega = \sum \omega(|F_o| - |F_c|)^2 + S\sum_j \epsilon_j + \sum_h \lambda_h G_h$$

The first summation in Ω ensures the optimum agreement between the observed (F_o) and the calculated (F_c) X-ray structure amplitudes. The reflections below the observational threshold are also included in the structure analysis, and details are given in ref 9. The observed structure amplitudes (*Fo*) obtained for the Cp fraction of *B. mori* (Table 2) [9] were used because of no significant difference of X-ray diffraction patterns between the Cp fraction of *B. mori* and $(AG)_{15}$ peptide.[27] The ω is the weight of each reflection. The second ensures the optimization of noncovalent interatomic interactions (ϵ_j). S is the scale factor used to adjust the overall weight of the second term with respect to the first. The third imposes, by the method of Lagrange undetermined multipliers (λ_h), the exact constraints (G_h) we have chosen. Atomic scattering factors for calculating structure factors were obtained using the method and values given in *International Tables for X-ray Crystallography*.[32]

Results

1. IR and ^{13}C CP/MAS NMR Spectra of $(AG)_{15}$ with Silk I Form. The IR and ^{13}C CP/MAS NMR spectra (0−68 ppm) of nonlabeled $(AG)_{15}$ in the silk I form were shown together with those spectra of *B. mori* silk fibroin with the silk I form in Figure 1. The assignments of the IR spectra for the silk I form have already been reported.[12] The IR pattern is the same between $(AG)_{15}$ and *B. mori* silk fibroin with silk I form, although the latter is slightly broader, indicating that $(AG)_{15}$ becomes a model of silk I. The ^{13}C chemical shifts of main peaks of Ala Cα and Cβ carbons, and Gly Cα carbon are in agreement between $(AG)_{15}$ and the silk fibroin, indicating the peptide, $(AG)_{15}$, in the silk I form can be used for the silk I model of the silk fibroin. The homogeneous structure of the peptide in the silk I form is easily suggested from the sharp single peak of Ala Cβ carbon. This is in contrast with the corresponding broad and asymmetric Ala Cβ peak of the peptide in the silk II form, which reflects a heterogeneous structure. In the spectrum of *B. mori* silk fibroin, the Ala Cβ peak is slightly broader due to the presence of Ala residues with basically random coil form in semicrystalline regions such as VGAGY, or an amorphous region such as YVANG in the heavy chain of *B. mori* silk fibroin, although Ala residues are mainly in the crystalline region such as $(GAGAGS)n$.[33,34]

2. Determination of the Torsion Angles of the Ala^{15} and Gly^{16} Residues in $(AG)_{15}$ with Both 2D Spin-Diffusion NMR and REDOR. Figure 2 shows the 2D spin-diffusion NMR spectrum of $(AG)_6A[1\text{-}^{13}C]G^{14}[1\text{-}^{13}C]A^{15}G(AG)_7$ together with the simulated spectrum for determination of the torsion angle of Ala^{15}

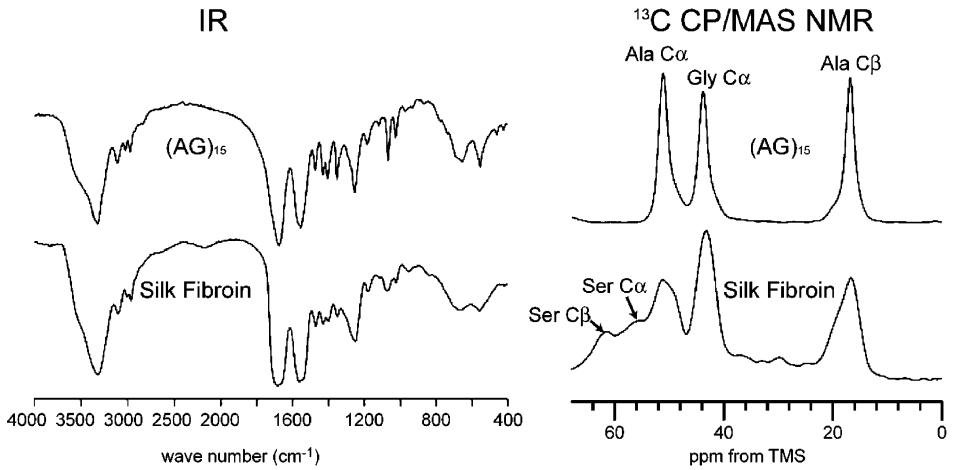

Figure 1. IR and ^{13}C CP/MAS NMR (0−68 ppm) spectra of $(AG)_{15}$ and *Bombyx mori* silk fibroin in silk I forms.

Table 2. Observed (I*obs*) and Calculated (I*cald*) Structure Amplitudes for the *β*-turn Type II Structure as the Model for Silk I Obtained Here

data no.	(*hkl*)	I*obs*	I*cald*	data no.	(*hkl*)	I*obs*	I*cald*	data no.	(*hkl*)	I*obs*	I*cald*
1	(011)	75	89	11	(122)	76	75	17	(043)	121	100
	(020)								(201)		
				12	(013)	49	20		(211)		
2	(021)	42	45		(140)				(004)		
									(220)		
3	(002)	151	164	13	(042)	115	108		(133)		
	(110)				(023)				(014)		
					(051)						
4	(012)	93	81		(141)			18	(221)	68	83
	(031)				(132)				(152)		
	(101)								(160)		
				14	(033)	58	46				
5	(111)	32	79		(103)			19	(230)	70	47
	(120)				(113)				(062)		
									(024)		
6	(022)	37	42	15	(150)	142	144				
					(052)			20	(161)	105	116
7	(121)	156	128		(142)				(231)		
	(040)				(060)				(202)		
					(151)				(212)		
8	(130)	42	35		(123)				(053)		
	(041)				(200)				(043)		
9	(032)	43	49	16	(210)	63	36	21	(034)	74	63
	(102)				(061)				(104)		
									(071)		
10	(112)	122	129								
	(131)										

residue. In our previous paper,[26] we determined the torsion angles of Ala^{15} residue as $(\phi, \psi) = (-60°, 130°)$, but the determination was performed by checking the degree of the agreement between the observed and simulated spectra with eye. In this paper, a more rigorous determination will be performed with RMSD map mentioned above. The RMSD map for the determination of torsion angles of Ala^{15} residue calculated from the difference in the observed and calculated 2D spin-diffusion NMR spectra was prepared in the range of $\phi = -80-0°$ and $\psi = 80-140°$ as shown in Figure 3. There are two minima, $(\phi, \psi) = (-60°, 120°)$ and $(-30°, 100°)$, marked by black circles, and therefore, a further determination of the torsion angles is required. Because the internuclei atomic distance between the carbonyl carbon of Gly^{14} residue and amide nitrogen of Gly^{16} residue changes as a function of the torsion angles, ϕ and ψ of Ala^{15} residue, such an atomic distance determined with the REDOR experiment can be used for a further determination. The contour lines of the distances, including experimental errors, are shown in Figure 4. The atomic distance between [1-^{13}C]Gly^{14} and [^{15}N]Gly^{16} for the sample R3, which gives the information of the torsion angles ϕ and ψ of Ala^{15} residue, was reported to be 3.8 ± 0.1 Å.[26] Thus, $(\phi, \psi) = (-30°, 100°)$ was clearly excluded and $(-60°, 120°)$ was selected in Figure 4. The 2D spin-diffusion spectrum calculated for $(\phi, \psi) = (-60°, 120°)$ was shown in Figure 2; an agreement between the observed and calculated spectra was good. The torsion angle determined here is close to the torsion angles $(\phi, \psi) = (-60°, 130°)$ reported previously.[26]

Next, for determination of other torsion angles of Gly^{16} residue, the RMSD map of the 2D spin-diffusion NMR spectrum of $(AG)_7$[1-^{13}C]A^{15}[1-^{13}C]$G^{16}(AG)_7$ (Figure 2) was also calculated and shown in Figure 5. There are four minima, $(\phi, \psi) = (70°, 10°)$, $(100°, 0°)$, $(120°, -50°)$, and $(100°, -60°)$, marked by black circles. The atomic distance between [1-^{13}C]Ala^{15} and [^{15}N]Ala^{17} for the sample R4, which gives the information on the

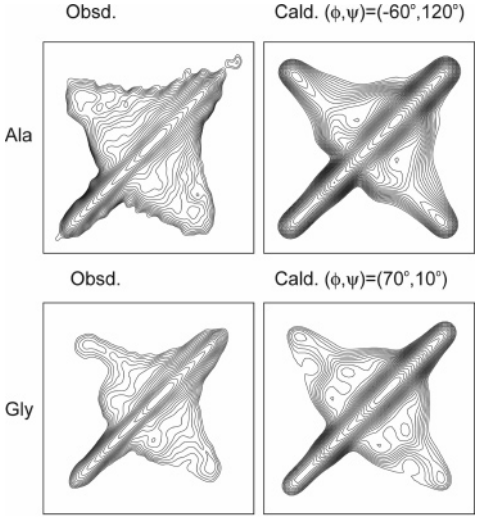

Figure 2. 2D spin-diffusion NMR spectra of $(AG)_6A[1\text{-}^{13}C]\text{-}G^{14}[1\text{-}^{13}C]A^{15}G(AG)_7$ and $(AG)_7[1\text{-}^{13}C]A^{15}[1\text{-}^{13}C]G^{16}(AG)_7$ for determinations of the torsion angles $Ala^{15}(\phi, \psi)$ and $Gly^{16}(\phi, \psi)$ in $(AG)_{15}$, respectively. Left: observed. Right: calculated. Details are described in the text.

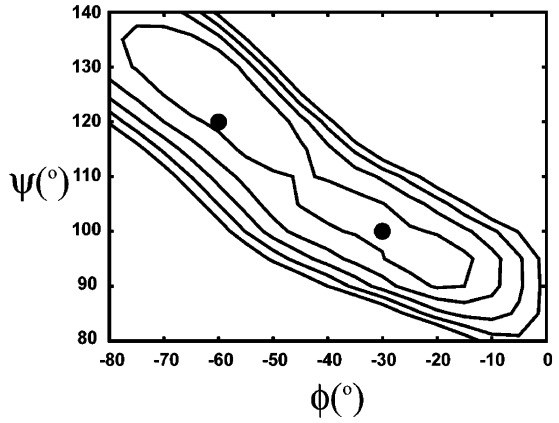

Figure 3. RMSD map for the determination of the torsion angles, $Ala(\phi, \psi)$, from the 2D spin-diffusion NMR spectrum of $(AG)_6A[1\text{-}^{13}C]G^{14}[1\text{-}^{13}C]A^{15}G(AG)_7$. Two minima (●) were obtained at $Ala(\phi, \psi) = (-60°, 120°)$ and $Ala(\phi, \psi) = (-30°, 100°)$.

torsion angles ϕ and ψ of Gly^{16} residue determined from the REDOR experiment, was reported to be 3.2 ± 0.1 Å.[26] Thus, in Figure 4, it seems possible to rule out $(\phi, \psi) = (120°, -50°)$, but the other three torsion angles cannot be excluded. A further determination was performed by the use of 2D spin-diffusion NMR spectrum of $(AG)_6A[1\text{-}^{13}C]G^{14}A[1\text{-}^{13}C]G^{16}(AG)_7$. When the torsion angles of Ala^{15} residue was set as $(\phi, \psi) = (-60°, 120°)$ as mentioned above, the spectral pattern depends on only the torsion angles, ϕ and ψ of Gly^{16} residue. The calculated spectra for three torsion angles are shown in Figure 6 together with the observed spectrum. The torsion angles $(\phi, \psi) = (100°, -60°)$ can be clearly excluded, but it seems difficult to distinguish the torsion angles $(\phi, \psi) = (70°, 10°)$ or $(\phi, \psi) = (100°, 0°)$. Thus, the latter two sets of the torsion angles will be used as initial torsion angles of the Gly residue for a further calculation with X-ray diffraction data in the next section.

3. Combination of ^{13}C CP/MAS NMR and X-ray Diffraction Analysis for Determination of Silk I Structure. X-ray diffraction data of the crystalline fraction of *B. mori* silk fibroin have been reported by

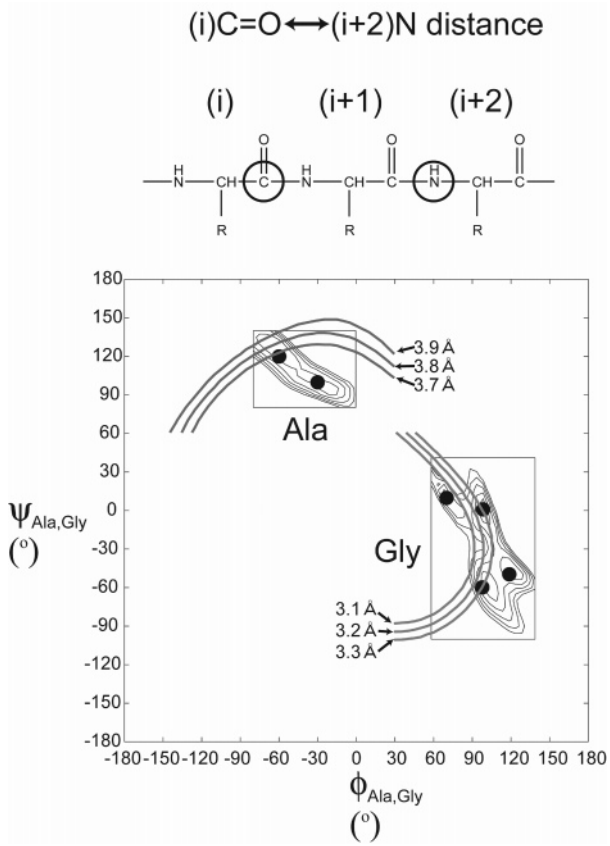

Figure 4. Determination of the torsion angles, $Ala^{15}(\phi, \psi)$ and $Gly^{14}(\phi, \psi)$ in $(AG)_{15}$, from both 2D spin-diffusion NMR and REDOR data. Details are described in the text.

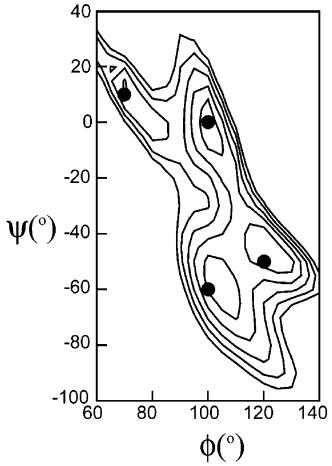

Figure 5. RMSD map for the determination of the torsion angles, $Gly^{16}(\phi, \psi)$ from 2D spin-diffusion NMR spectrum of $(AG)_7[1\text{-}^{13}C]A^{15}[1\text{-}^{13}C]G^{16}(AG)_7$. There are four minima, $(\phi, \psi) = (70°, 10°)$, $(100°, 0°)$, $(120°, -50°)$, and $(100°, -60°)$, marked by black circles (●).

Okuyama et al.;[9] the unit cell was orthorhombic and the space group was $P2_12_12_1$, and the lattice constants were $a = 4.65$ Å, $b = 14.24$ Å, and $c = 8.88$ Å, $\alpha = \beta = \gamma = 90°$. There are four repeated units, Ala-Gly, in a unit cell. And two 2_1-helix chains are included with antiparallel forms in a unit cell. By taking into account the (ϕ, ψ) values of the Gly and Ala residues determined for a poly(AG) chain using solid-state NMR and the X-ray diffraction data, the structure of silk fibroin chains with silk I form was calculated by including intermolecular chain arrangement. The initial torsion angle

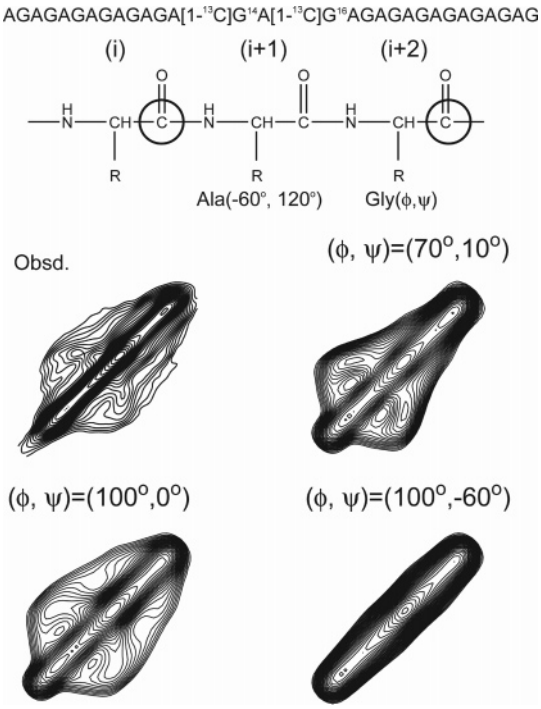

Figure 6. 2D spin-diffusion NMR spectrum of $(AG)_6A[1\text{-}^{13}C]\text{-}G^{14}A[1\text{-}^{13}C]G^{16}(AG)_7$. The torsion angles of Ala^{15} residue were set as $(\phi, \psi) = (-60°, 120°)$, and therefore, the spectral pattern depends on only the torsion angles ϕ and ψ of Gly^{16}. The calculated spectra for three torsion angles, $(\phi, \psi) = (70°, 10°)$, $(100°, 0°)$, and $(100°, -60°)$ selected in Figure 5 are shown.

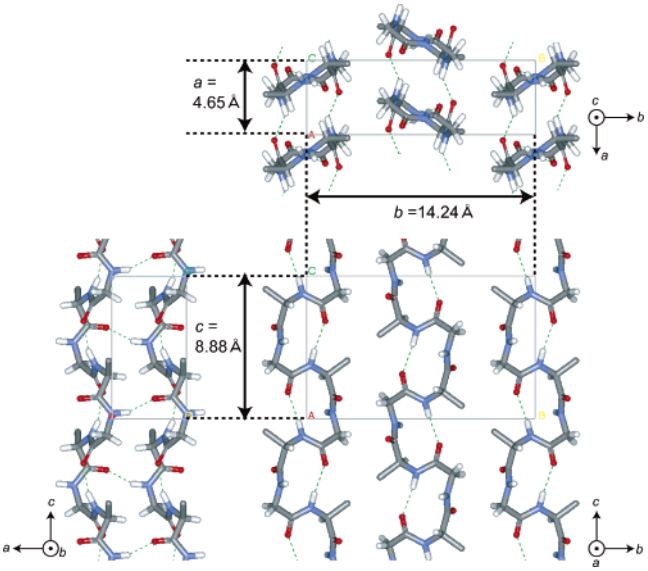

Figure 7. Packing structure of poly(AG) chains with β-turn type II conformation as a model for silk I after linked-atom least-squares (LALS) calculation. Dotted lines denote hydrogen bonds.

for linked-atom least-squares (LALS) calculation is $(\phi, \psi) = (-60°, 120°)$ for Ala residue, but there are two candidates, $(\phi, \psi) = (70°, 10°)$ or $(\phi, \psi) = (100°, 0°)$, for Gly residue. After LALS calculation described in the Materials and Methods Section, the same set of the torsion angles that satisfies X-ray diffraction data was obtained with an R factor of 10%; $(\phi, \psi) = (-62°, 125°)$ for Ala residue and $(\phi, \psi) = (77°, 10°)$ for Gly residue independent of the initial sets of the torsion angles of Gly residues as summarized in Tables 2 and 3. The intermolecular arrangement of poly(AG) chains prepared with the structural data in Table 3 is shown in Figure 7. These are basically the same as the previous model proposed by us.[26] The conformation of one silk I chain is a repeated β-turn type II that is capable of forming intramolecular hydrogen bonds (viewed along the *bc* direction). The geometry of the intramolecular hydrogen bond is normal, both in terms of length (N···O; 3.0 Å) and angle (∠N···O−C; 129°). In addition, there are intermolecular hydrogen bonds whose direction is perpendicular to the fiber axis. This is clear in the view from the *ac* plane. The geometry of the intermolecular hydrogen bond is the length, N···O; 2.82 Å, and the angle, ∠N···O−C; 152°. Thus, there are intra- and intermolecular hydrogen bonds alternatively along one chain in this model.

Table 3. Refinement Details for the β-turn Type II Structure for the Model of Silk I Obtained Here with Ala-Gly Repeating Unit

torsion angle (°)	
ϕ_{Ala}	−62
ψ_{Ala}	125
ω_{Ala}	180
ϕ_{Gly}	77
ψ_{Gly}	10
ω_{Gly}	177
Eulerian angle (°)	
ϵ_x	114
ϵ_y	27
ϵ_z	139
other parameters	
S (Å)	−0.92
μ (°)	87.3
w	0.308
scale factor	1.61
attenuation factor	3.48
hydrogen bonds	
intermolecular N(G)— O(Ala), between parallel	
distance (Å)	2.82
angle[a](°)	152
intramolecular N(Ala)—O(Gly)	
distance (Å)	3.0
angle (°)[a]	129

R-factors[b]	excl rej-unobs	excl unobs
normal	10.42	9.67
weighted quadratic	12.04	11.60
weighted normal	10.42	9.67

[a] Here the angle refers to ∠N···O−C. [b] Details of the R-factors calculation are given in ref 9.

4. Examination of the β-Turn Type II Structure with REDOR Observation. Seven kinds of both ^{13}C and ^{15}N labeled $(AG)_{15}$ samples, R1−R7, were synthesized for REDOR experiments, and the labeling sites were summarized in Figure 8. The R5 sample was used to determine the atomic distance between $[1\text{-}^{13}C]Gly^{14}$ and $[^{15}N]Ala^{17}$, which was very effective to identify the β-turn conformation through the determination of the distance of intramolecular hydrogen bonding. The REDOR observations of the samples, R1 and R2, give the information on ψ angles of Ala^{15} and Gly^{16} residues, respectively. The information on both ψ angle of Ala^{15} and ϕ angle of Gly^{16} is also obtained from REDOR experiment of the sample R6. The REDOR data of sample R7, the atomic distance between $[^{15}N]Gly^{14}$ and $[3\text{-}^{13}C]Ala^{17}$, give the information on the combination of ψ angle of Gly^{14}, ϕ and ψ angles of Ala^{15}, ϕ and ψ angles of Gly^{16}, and ϕ angle of Ala^{17}.

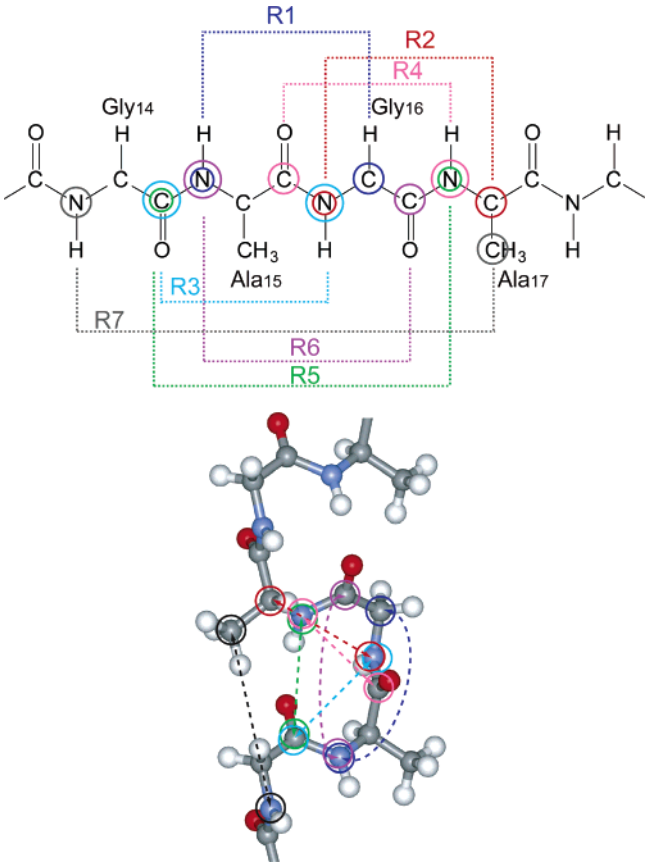

Figure 8. Several pairs of atomic distances between ^{13}C and ^{15}N nuclei in the ^{13}C,^{15}N labeled $(AG)_{15}$ samples for REDOR experiments.

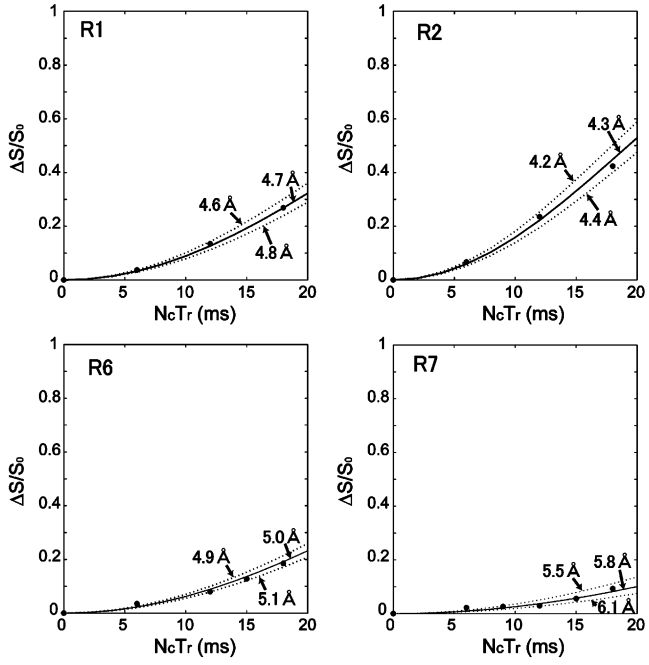

Figure 9. REDOR plots, $\Delta S/S_0$ vs N_cT_r, for the peptides R1, R2, R6, and R7 in Table 1.

The observed plots of $\Delta S/S_{off}$ ($= 1 - S/S_{off}$) against N_cT_r (ms) of the samples R1, R2, R6, and R7 for atomic distance determinations with REDOR are summarized in Figure 9. The error in the distance determination is relatively large in the sample R7 ($\pm$ 0.3 Å), but others are $\pm$ 0.1 Å. The observed distances are listed in Table 1, together with the calculated ones, by assuming the silk I model reported here. The agreement is very good, supporting this structural model. For example, the atomic distance between [^{15}N]Gly^{14} and [3-^{13}C]Ala^{17} was 5.8 Å and relatively short because of the presence of intramolecular hydrogen bonding between [1-^{13}C]Gly^{14} and [^{15}N]Ala^{17}.

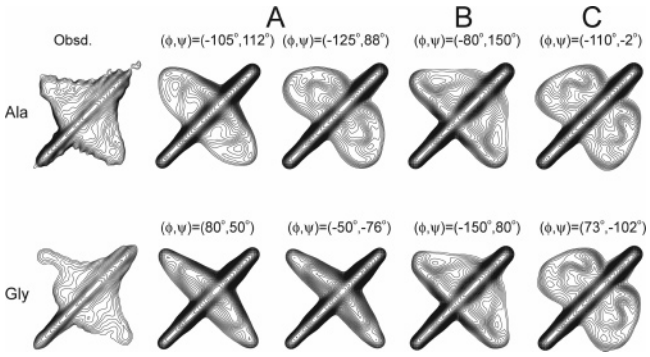

Figure 10. Observed and calculated 2D spin-diffusion NMR spectra of $(AG)_6A$[1-^{13}C]G^{14}[1-^{13}C]A^{15}G$(AG)_7$ and $(AG)_7$[1-^{13}C]-A^{15}[1-^{13}C]G$^{16}(AG)_7$ for determinations of the torsion angles Ala^{15}(ϕ, ψ) and Gly^{16}(ϕ, ψ) in $(AG)_{15}$, respectively. The calculations were performed for the structural models reported previously. A: Two models by Lotz and Keith.[7,8] B: Model by Fossey.[11] C: Model by Okuyama.[9]

5. Comparison of the Silk I Model Proposed Here with Other Models Proposed Previously. A number of models for silk I have been proposed.[7−11] At first, we will concentrate the silk I models by Lotz and Keith,[7,8] and Fossey et al.[11] In the "crankshaft model" of Lotz and Keith, the Ala residues are in a β-sheet conformation, and Gly residues in a left-handed or right-handed α-helical conformation, Ala ($\phi = -105°$ and $\psi = 112°$) and Gly ($\phi = 80°$ and $\psi = 50°$) or Ala ($\phi = -125°$ and $\psi = 88°$) and Gly ($\phi = -50°$ and $\psi = -76°$). The model proposed by Fossey *et al.* has right-handed and left-handed twisting of sheets, with approximately equal magnitudes of the twist, Ala ($\phi = -80°$and $\psi = 150°$) and Gly ($\phi = -150°$ and $\psi = 80°$). The 2D spin-diffusion NMR spectra calculated with these torsion angles are used for checking the previous models (Figure 10). By comparing the calculated and observed spectra, it is clear that the agreement is poor compared with the β-turn type II model proposed here (Figure 2). The observed chemical-shift values of Ala Cα, Cβ and Gly Cα carbons,[33,34] and REDOR data for silk I structure also support only the model proposed in this paper.

Recently, two further models of silk I have been proposed. He et al.[10] reported a silk I single-crystal diffraction pattern of *B. mori* silk fibroin. The modeling of their data suggests that a better fit is obtained by allowing either a slight twist of the 2-fold helix to a 12_5 helix or by producing a similar very slight contraction of the chain-extended conformation through the type of random torsion angle fluctuation. They did not report the torsion angles of Ala and Gly residues, and therefore, it is difficult to check the validity of their silk I model from the solid-state NMR data reported here. However, judging from the process for determination of silk I structure performed here, only this structural model seems to be a valid model. Okuyama *et al.*[9] reported the torsion angles of Ala and Gly residues of poly(AG) with only X-ray diffraction data used in this paper; Ala ($\phi = -110°$ and $\psi = -2°$) and Gly ($\phi = 73°$ and $\psi = -102°$) of poly(AG) with silk I form was finally reported. The agreement is not so good between the observed and calculated 2D spin-diffusion NMR spectra

when these torsion angles are used (Figure 10).

In the structural determination of silk I with solid-state NMR, combination of spin-diffusion NMR, REDOR as well as the quantitative use of the chemical-shift data coupled with chemical-shift contour plots seems useful and gives enough amounts of the structural constraints. Even if the conformation of the single chain was determined correctly by such a combination of several solid-state NMR techniques, it is still difficult to construct the correct structural model with intermolecular arrangement. Thus, it seems important to use X-ray diffraction data for the purpose. This paper seems a nice example to determine the detailed silk I structure with intermolecular arrangement by the use of several solid-state NMR and X-ray diffraction methods complementarily.

The role of water molecules is very important in the generation of silk I structure and structural transition from silk I to silk II as reported previously.[10,23−25,35−38] We prepared the conformational probability maps using molecular dynamic (MD) simulations of three model dipeptides of the type Ac-Xaa-NHMe, (where Xaa = Gly, Ala, and Ser) in explicit water and discussed the structure of these residues in water.[37] The conformational probability maps constructed for these dipeptides indicated that the previous torsion angles, $(\phi, \psi) = (-60°, 130°)$ for Ala and Ser residues, and $(\phi, \psi) = (70°, 30°)$ for Gly residue, in the type II β-turn structure were in the stable state in water, and only the silk I model proposed by us[26] could satisfy the stable state for these residues simultaneously among silk I models proposed previously. The torsion angles determined in this work are $(\phi, \psi) = (-62°, 125°)$ for Ala residue and $(\phi, \psi) = (77°, 10°)$ for Gly residue and are slightly different from the previous angles $(\phi, \psi) = (-60°, 130°)$ for Ala residue and $(\phi, \psi) = (70°, 30°)$ for Gly residue. However, this is only a very small difference, and the conclusion in the previous paper[37] is still valid. Similarly, the silk I structure determined here can explain the structural transition from silk I to silk II as studied previously in detail.[38]

Acknowledgment. T.A. acknowledges research grant support from the Asahi Glass Foundation, Japan and Grant-in Aid for Scientific Research by the Ministry of Education, Culture, Sports, Science, and Technology of Japan (no.16350121).

References and Notes

(1) Asakura, T.; Kaplan, D. L. In *Encyclopedia of Agricultural Science*; Arutzen, C. J., Ed.; Academic Press: New York, 1994; Vol. 4, pp 1−11.
(2) Shimura, K., In *Zoku Kenshi no Kozo (Structure of Silk Fibers)*; Hojyo, N., Ed.; Shinshu University: Ueda, Japan, 1980; pp 335−352.
(3) Mita, K.; Ichimura, S.; James, C. T. *J. Mol. Evol.* **1994**, *38*, 583−592.
(4) Zhou, C.; Confalonieri, F.; Medina, N.; Zivanovic, Y.; Esnault, C.; Yang, T.; Jacquet, M.; Janin, J.; Duguet, M.; Perasso, R.; Li, Z. *Nucleic Acids Res.* **2000**, *28*, 2413−2419.
(5) Fraser, R. D. B.; MacRae, T. P., In *Conformations of Fibrous Proteins and Related Synthetic Polypeptides*; Academic Press: New York, 1973.
(6) Takahashi, Y.; Gehoh, M.; Yuzuriha, K. *Int. J. Biol. Macromol.* **1999**, *24*, 127−38.
(7) Lotz, B.; Cesari, C. F. *Biochimie* **1979**, *61*, 205−214.
(8) Lotz, B.; Keith, D. H. *J. Mol. Biol.* **1971**, *61*, 201−215.
(9) Okuyama, K.; Somashekar, R.; Noguchi, K.; Ichimura, S. *Biopolymers* **2001**, *59*, 310−319.
(10) He, S.-J.; Valluzzi, R.; Gido, S. P. *Int. J. Biol. Macromol.* **1999**, *24*, 187−195.
(11) Fossey, A. S.; Nemethy, G.; Gibson, D. K.; Scheraga, A. H. *Biopolymers* **1991**, *31*, 1529−1541.
(12) Asakura, T.; Kuzuhara, A.; Tabeta, R.; Saito, H. *Macromolecules* **1985**, *18*, 1841−5.
(13) Saito, H.; Tabeta, R.; Asakura, T.; Iwanaga, Y.; Shoji, A.; Ozaki, T.; Ando, I. *Macromolecules* **1984**, *17*, 1405−12.
(14) Saito, H.; Iwanaga, Y.; Tabeta, R.; Narita, M.; Asakura, T. *Chem Lett.* **1983**, 427−430.
(15) Asakura, T.; Yamaguchi, T. *Nippon Sanshigaku Zasshi* **1987**, *56*, 300−304.
(16) Ishida, M.; Asakura, T.; Yokoi, M.; Saito, H. *Macromolecules* **1990**, *23*, 88−94.
(17) Nicholson, L. K.; Asakura, T.; Demura, M.; Cross, T. A. *Biopolymers* **1993**, *33*, 847−861.
(18) Asakura, T.; Aoki, A.; Demura, M.; Joers, J. M.; Rosanske, R. C.; Guillion, T. *Polym. J.* **1994**, *26*, 1405−1408.
(19) Asakura, T.; Demura, M.; Hiraishi, Y.; Ogawa, K.; Uyama, A. *Chem. Lett.* **1994**, 2249−52.
(20) Demura, M.; Minami, M.; Asakura, T.; Cross, T. A. *J. Am. Chem. Soc.* **1998**, *120*, 1300−1308.
(21) Asakura, T.; Yao, J.; Yamane, T.; Umemura, K.; Ulrich, A. S. *J. Am. Chem. Soc.* **2002**, *124*, 8794−8795.
(22) Asakura, T.; Yao, J. *Protein Sci.* **2002**, *11*, 2706−2713.
(23) Asakura, T. *Macromol. Chem.* **1986**, *7*, 755−759.
(24) Asakura, T.; Ashida J.; Yamane T. In *NMR Spectroscopy and Polymers in Solution and in the Solid State*; Cheng H. N., English A. D., Eds.; American Chemical Society: Washington, DC, 2002; pp 71−82.
(25) Zhao, C.; Asakura, T. *Prog. Nucl. Magn. Reson. Spectrosc.* **2001**, *39*, 301−352.
(26) Asakura, T.; Ashida, J.; Yamane, T.; Kameda, T.; Nakazawa, Y.; Ohgo, K.; Komatsu, K. *J. Mol. Biol.* **2001**, *306*, 291−305.
(27) Asakura, T.; Yamane, T.; Nakazawa, Y.; Kameda, T.; Ando, K. *Biopolymers* **2001**, *58*, 521−525.
(28) Gullion, T.; Kishore, R.; Asakura, T. *J. Am. Chem. Soc.* **2003**, *125*, 7510−7511.
(29) Gullion, T.; Schaefer, J. *J. Magn. Reson.* **1991**, *92*, 439−42.
(30) Weliky, D. P.; Bennett, A. E.; Zvi, A.; Anglister, J.; Steinbach, P. J.; Tycko, R. *Nat. Struct. Biol.* **1999**, *6*, 141−145.
(31) Smith, P. J. C.; Arnott, S. *Acta Crystallogr.* **1978**, *A34*, 3−11.
(32) *International Tables for X-ray Crystallography*; Kynoch Press: Birmingham, UK, 1974; Vol. 4, p 71.
(33) Asakura, T.; Sugino, R.; Yao, J.; Takashima, H.; Kishore R. *Biochemistry* **2002**, *41*, 4415−4424.
(34) Asakura T.; Ohgo, K.; Ishida, T.; Taddei, P.; Monti, P.; Kishore, R. *Biomacromolecules* **2005**, *6*, 468−474.
(35) Rössle, M.; Panine, P.; Urban, V. S.; Riekel, C. *Biopolymers* **2004**, *74*, 316−327.
(36) Sohn, S.; Strey, H. H.; Gido, S. P. *Biomacromolecules* **2004**, *5*, 751−757.
(37) Yamane, T.; Umemura, K.; Asakura, T. *Macromolecules* **2002**, *35*, 8831−8838.
(38) Yamane, T.; Umemura, K.; Nakazawa, Y.; Asakura, T. *Macromolecules* **2003**, *36*, 6766−6772.

MA050936Y